Supplement of Atmos. Meas. Tech., 14, 715–736, 2021
https://doi.org/10.5194/amt-14-715-2021-supplement

Atmospheric Measurement Techniques
Open Access
EGU

Supplement of

New in situ aerosol hyperspectral optical measurements over 300–700 nm – Part 2: Extinction, total absorption, water- and methanol-soluble absorption observed during the KORUS-OC cruise

Carolyn E. Jordan et al.

Correspondence to: Carolyn E. Jordan (carolyn.jordan@nasa.gov)

Table S1. Filter number, sampling interval, mean location with standard deviation, and flags for the absorption spectra (-8888 = below detection; -9999 = missing). There were no flags needed for the filter mean SpEx extinction spectra. Gray font indicates filters excluded from analyses due to ship exhaust plume contamination (see below).

	Date & Time (KST)		Latitude (°N)		Longitude (°E)		Flags		
Filter Number	Start	Stop	Mean	St. Dev.	Mean	St. Dev.	Total Abs.	DI-soluble Abs.	MeOH-soluble Abs.
1	5/22/16 6:22	5/22/16 9:08	37.0115	0.0052	130.7049	0.0044			
2	5/22/16 9:10	5/22/16 12:14	37.0291	0.0052	130.7205	0.0107			
3	5/22/16 12:15	5/22/16 15:25	37.0329	0.0043	130.7496	0.0066			
4	5/22/16 15:27	5/22/16 18:21	37.0241	0.0071	130.7712	0.0163			
5	5/22/16 18:23	5/23/16 6:35	36.9782	0.0213	130.8028	0.0192			
6	5/23/16 6:39	5/23/16 9:21	37.2664	0.1088	131.1076	0.1130			-9999
7	5/23/16 9:23	5/23/16 12:14	37.5483	0.0452	131.3533	0.0298			-9999
8	5/23/16 12:15	5/23/16 15:21	37.7078	0.0534	131.2631	0.0322			-9999
9	5/23/16 15:22	5/23/16 17:55	37.8527	0.0391	131.1205	0.0399			-9999
10	5/24/16 6:26	5/24/16 9:19	37.0772	0.0103	131.0734	0.0906			-9999
11	5/24/16 9:21	5/24/16 12:10	37.1090	0.0117	130.8724	0.0820			
12	5/24/16 12:12	5/24/16 15:13	37.1455	0.0095	130.6959	0.0826			-9999
13	5/24/16 15:14	5/24/16 18:16	37.1934	0.0376	130.4023	0.1285			
14	5/24/16 18:18	5/25/16 6:20	37.5795	0.1009	129.9108	0.1136			-9999
15	5/25/16 6:23	5/25/16 9:12	37.6988	0.0126	129.7585	0.0434			
16	5/25/16 9:13	5/25/16 12:01	37.6856	0.0086	129.6430	0.0125			-9999
17	5/25/16 12:02	5/25/16 15:01	37.7793	0.0332	129.6209	0.0160			-9999
18	5/25/16 15:03	5/25/16 17:54	37.8287	0.0090	129.5813	0.0168			-9999
19	5/25/16 17:55	5/26/16 6:20	37.5098	0.4201	129.7468	0.2728			-9999
20	5/26/16 6:23	5/26/16 9:24	36.5316	0.0061	130.2587	0.0322			
21	5/26/16 9:25	5/26/16 12:13	36.4911	0.0376	130.1324	0.0464			
22	5/26/16 12:14	5/26/16 15:08	36.4278	0.0289	130.0288	0.0588			
23	5/28/16 9:33	5/28/16 12:26	34.0779	0.0494	128.1513	0.1000			-9999
24	5/29/16 6:49	5/29/16 9:27	35.0119	0.0107	125.0027	0.0030			-9999
25	5/29/16 9:29	5/29/16 12:22	35.0017	0.0060	124.9125	0.0685			
26	5/29/16 12:23	5/29/16 15:30	34.9889	0.0101	124.7036	0.0638			
27	5/29/16 15:31	5/29/16 18:31	35.1041	0.0299	124.5085	0.0545			
28	5/29/16 18:32	5/30/16 6:21	35.0589	0.0163	124.3375	0.0103			
29	5/30/16 6:23	5/30/16 9:08	35.0473	0.0238	124.3578	0.0111	-8888		
30	5/30/16 9:09	5/30/16 12:11	35.0244	0.0347	124.3456	0.0163			
31	5/30/16 12:12	5/30/16 15:08	35.0684	0.0072	124.3714	0.0041			-9999
32	5/30/16 15:09	5/30/16 18:08	35.0331	0.0106	124.3750	0.0081			-9999
33	5/30/16 18:09	5/31/16 6:16	35.2348	0.1810	124.5618	0.1827			-9999
34	5/31/16 6:17	5/31/16 9:07	35.6493	0.0300	124.9787	0.0295		-8888	
35	5/31/16 9:08	5/31/16 12:07	35.6675	0.0027	125.1055	0.0682		-8888	

36	5/31/16 12:08	5/31/16 15:08	35.6621	0.0037	125.3913	0.1176		-8888	-9999
37	5/31/16 18:24	6/1/16 6:20	36.3116	0.3670	125.4494	0.2323			
38	6/1/16 6:21	6/1/16 9:06	36.8974	0.0480	125.2866	0.0324			-9999
39	6/1/16 9:06	6/1/16 12:13	37.2150	0.1145	125.5746	0.0948			
40	6/1/16 12:13	6/1/16 15:08	37.3512	0.0042	125.6766	0.0101			-9999
41	6/1/16 15:09	6/1/16 18:00	37.3373	0.0065	125.6571	0.0138			
42	6/1/16 18:01	6/2/16 6:11	36.5614	0.5072	125.0593	0.3295			
43	6/2/16 6:13	6/2/16 9:09	35.4287	0.1008	124.3942	0.0681			
44	6/2/16 9:10	6/2/16 12:06	35.2375	0.0667	124.3276	0.0070			
45	6/2/16 12:07	6/2/16 15:10	35.0508	0.0669	124.3396	0.0044			-9999
46	6/2/16 15:11	6/2/16 18:04	34.8459	0.0738	124.3356	0.0083			
47	6/2/16 18:05	6/3/16 6:13	33.9574	0.4177	124.2784	0.0272			
48	6/3/16 6:15	6/3/16 9:08	33.4690	0.0084	124.2439	0.0123			
49	6/3/16 9:09	6/3/16 12:09	33.4798	0.0102	124.2032	0.0083			
50	6/3/16 12:10	6/3/16 15:07	33.5074	0.0052	124.2043	0.0092			-9999
51	6/3/16 15:08	6/3/16 17:51	33.4949	0.0091	124.2353	0.0079		-9999	-9999
52	6/3/16 17:51	6/4/16 6:14	33.4971	0.0377	124.1984	0.0370			
53	6/4/16 6:16	6/4/16 9:19	33.5051	0.0074	124.7797	0.2245	-8888	-8888	-9999

Ship plume influence on filter samples. In Part 1, ship exhaust plume interceptions were flagged (PF = 1 for plume interception, = 0 for ambient conditions) based on TAP absorption data and gas phase measurements (Jordan et al., 2020b). For the 53 filter pairs collected, 15 filter sampling intervals did not have any ship plume interceptions at all (PF = 0 throughout the interval). Little difference was observed in scattering between filter means calculated with and without PF=1 (green symbols for all data and PF = 0, respectively, top panel Fig. S1), due to the fleeting nature of the plume interceptions over the 3- or 12-hour sampling intervals and the relatively minor enhancement in scattering coefficients for PF = 1 periods versus PF = 0. However, larger differences were found in absorption for 8 filters due to much larger differences between ambient and ship plume aerosol absorption (Fig. S1, middle panel). Further, calculations of single scattering albedo (ω) showed that an additional 5 filters deviated considerably between the two calculations when scattering was small (Figs. S1 and S2). Taking a conservative approach, all 13 of these filters (Table S2) have been excluded from the data analyses discussed in Section 3, although they remain in the map shown in Fig. 1 and were used in the determination of the correction factor used to adjust the filter-based spectral absorption correction to match the TAP values as described in Section 2.3.

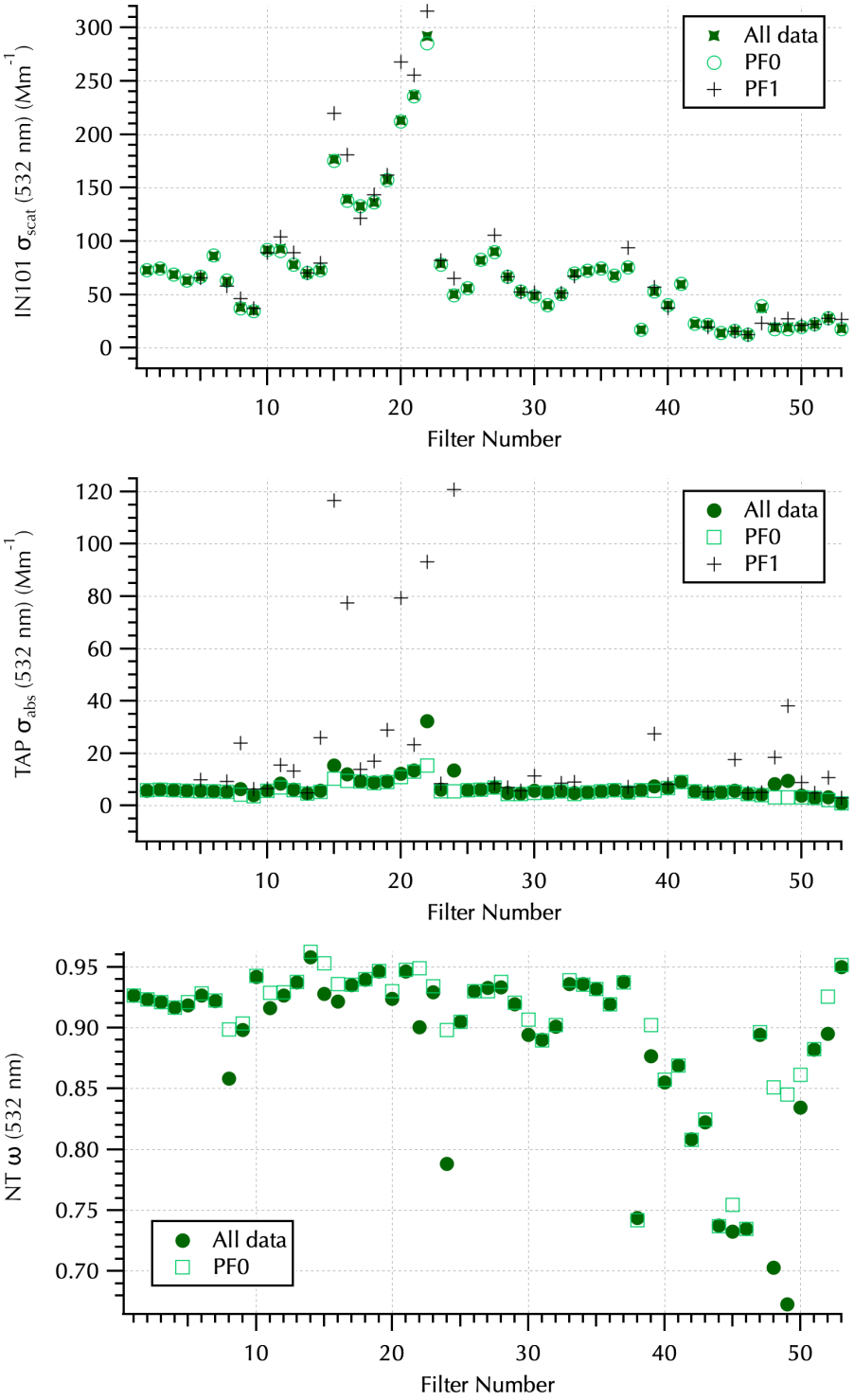

Figure S1. 532 nm σ_{scat} (top), σ_{abs} (middle), and ω (bottom) calculated for each filter sampling interval using all (PF = 0 and 1) data or just PF = 0 (solid and open green markers, respectively) or PF = 1 data (black plus symbols, top 2 panels only) from the IN101 nephelometer and TAP (denoted NT when used for σ_{ext} or ω calculations) instruments.

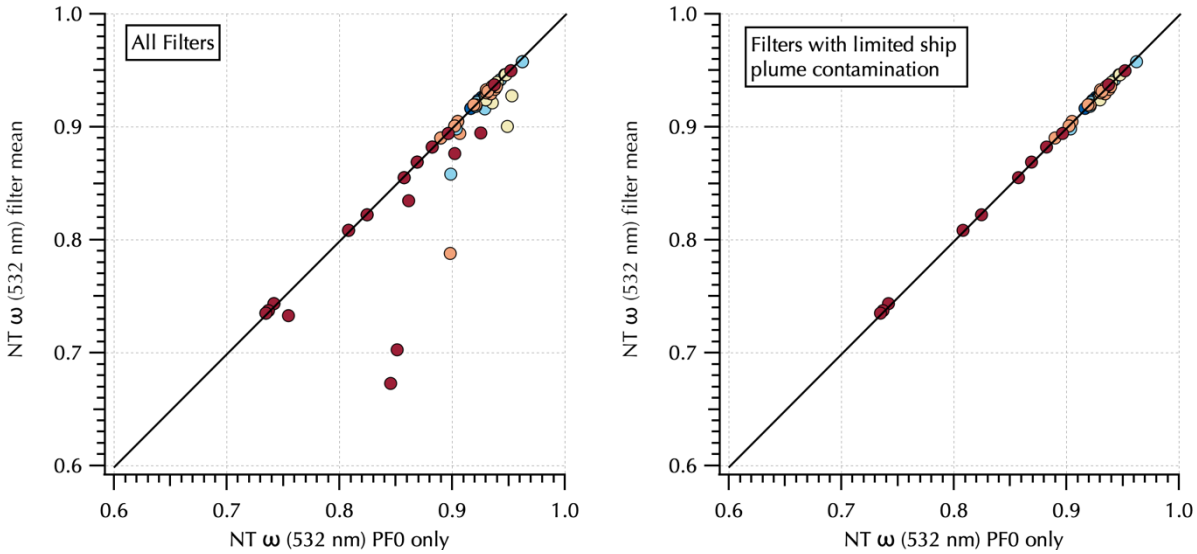

Figure S2. NT ω(532nm) calculated using all data over the filter sampling interval vs. using only PF = 0. All filters are shown (left panel), along with only those retained for further analyses (right panel).

Table S2. Filters excluded from further analyses (except as noted above) based on difference in NT ω calculated using PF = 0 only and PF = 0 and 1.

Meteorological Periods	**Filter Numbers**	**Ship Contaminated Filters**	**% Removed**
Stagnant	1-4	--	0
transition	5-14	8, 11	20
Transport/Haze - East	15-22	15, 16, 22	37.5
Transport/Haze - West	23-36	24, 30	14.3
Blocking	37-53	39, 45, 48, 49, 50, 52	35.3
Total	*53*	*13*	*24.5*

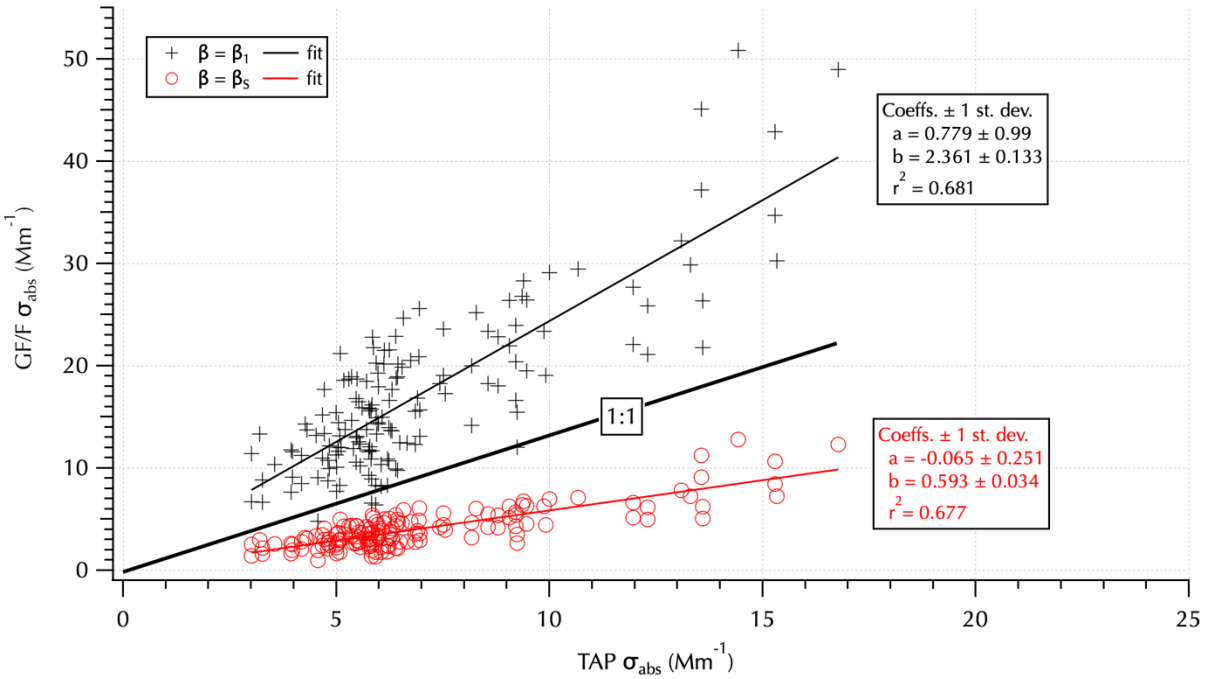

Figure S3. Comparison of σ_{abs} between GF/F and TAP measurements without any correction applied to the GF/F measurements (β_1, black pluses and line fit) and corrected using β_S (red circles and line fit). The 1:1 line (thick black line) is shown for comparison.

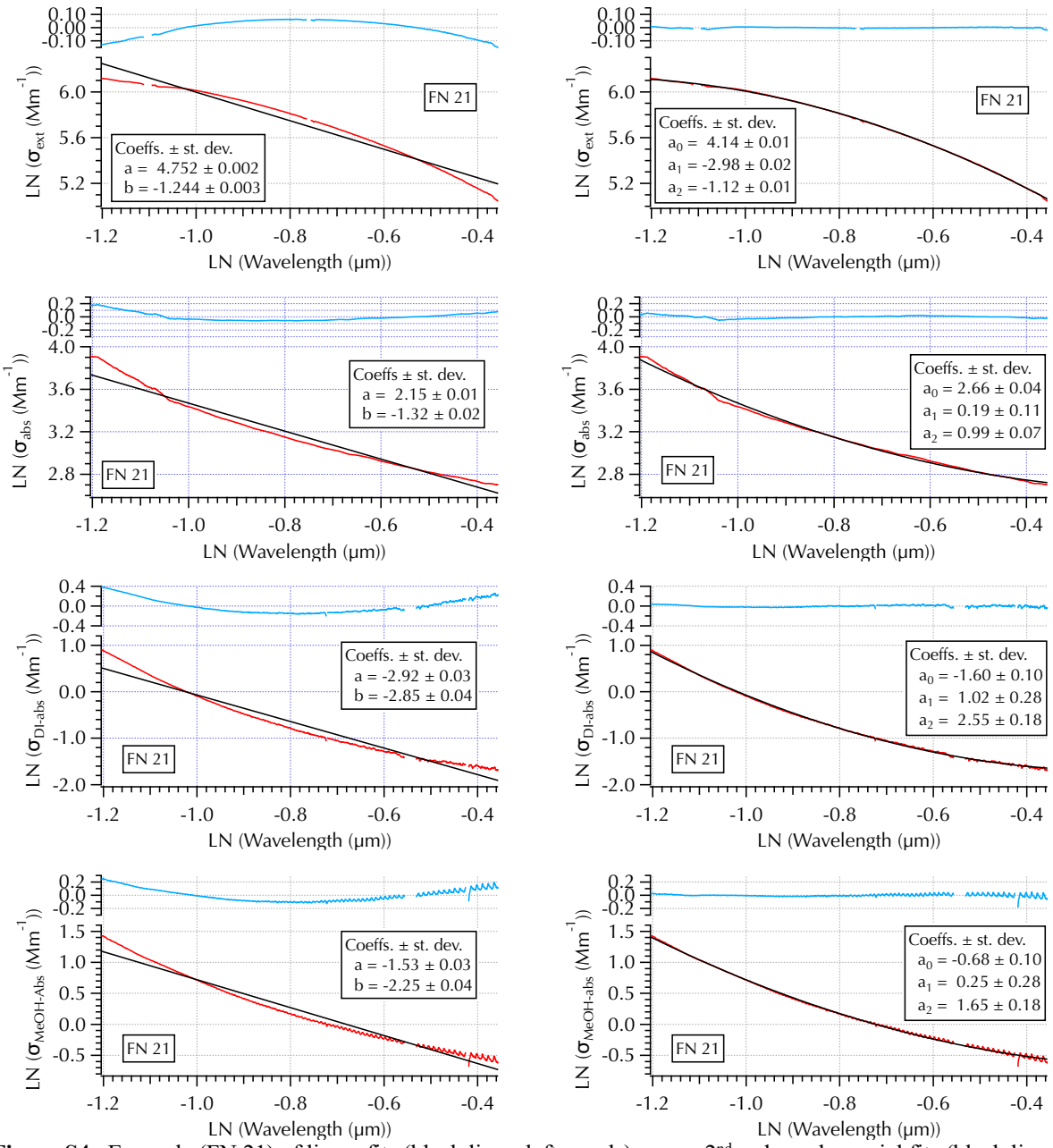

Figure S4. Example (FN 21) of linear fits (black lines, left panels) versus 2nd order polynomial fits (black lines, right panels) to measured spectra (red curves, all panels): σ_{ext} (top row), σ_{abs} (2nd row), $\sigma_{DI\text{-}abs}$ (3rd row), and $\sigma_{MeOH\text{-}abs}$ (bottom row). The residuals from each fit (blue curves) are shown above each curve fit. Note, FN21 was the example used in Fig. 2 for the Transport/Haze - East case. The x-axis labels of -1.2, -1.0, -0.8, -0.6 and -0.4 for LN(λ(μm)) equal 0.301, 0.368, 0.449, 0.549, 0.670, and 0.698 um wavelengths, respectively.

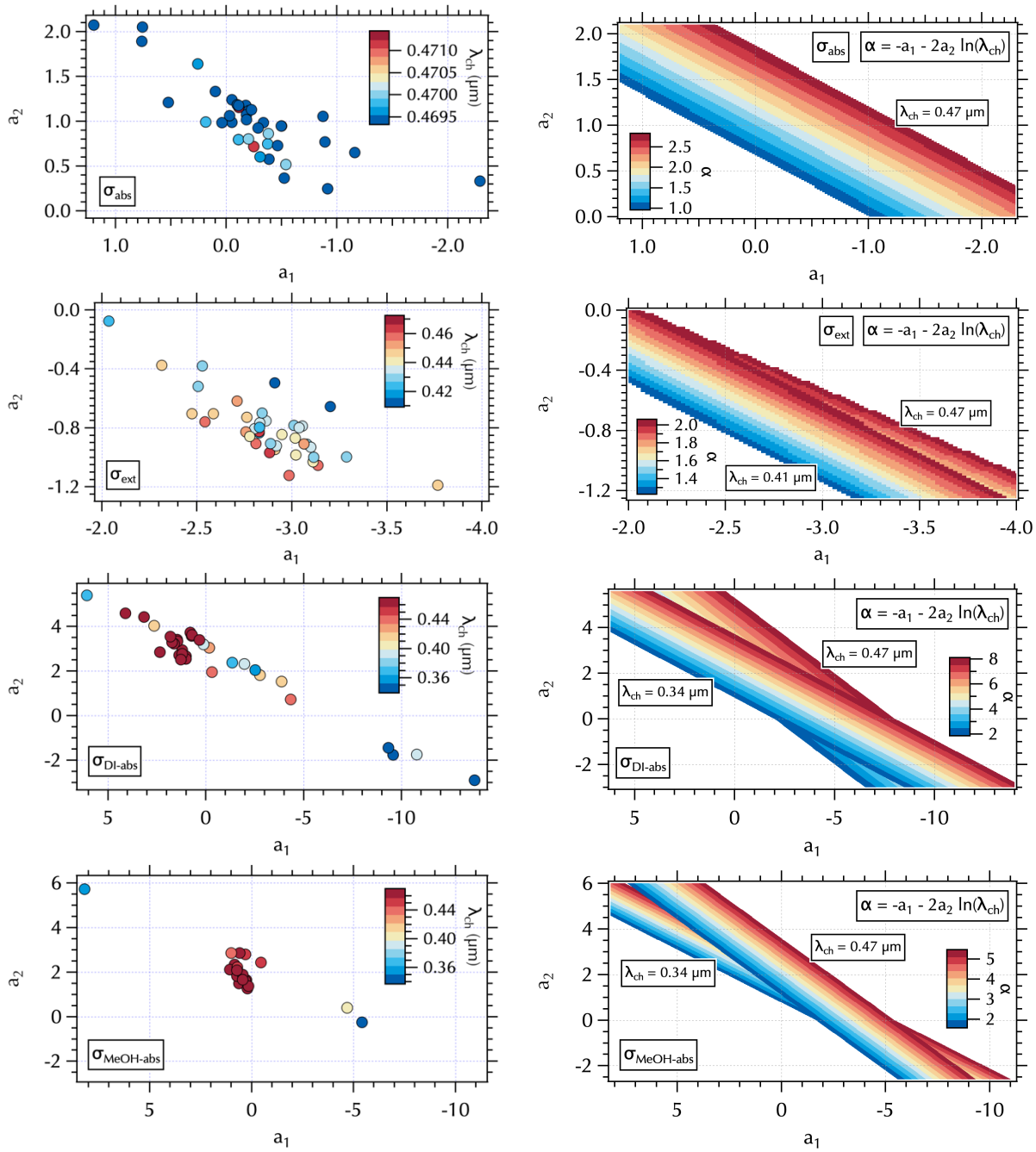

Figure S5. Maps of λ_{ch} (left panels) and the α (right panels) in a_2 vs. a_1 space for the range of values obtained from σ_{abs} (top row), σ_{ext} (2nd row), $\sigma_{DI\text{-}abs}$ (3rd row), and $\sigma_{MeOH\text{-}abs}$ (bottom row) spectra. The mapping of α in a_2 vs. a_1 space rotates as a function of λ_{ch} such that a narrow range (e.g. $\lambda_{ch}(\sigma_{abs}) = 0.47$, top left) maps to parallel lines in α (top right), while a wider range of values can map into a fan around $a_2 = 0$ (e.g., σ_{ext}, 2nd row) or distinct branches (e.g., $\sigma_{DI\text{-}abs}$ or $\sigma_{MeOH\text{-}abs}$, bottom 2 rows) compare the right panels here to the data shown in Fig. 7 of the main text. The color bars used in each of the α maps (right) match those of the Fig. 7 panels.